

**SYNTHESIS OF NOVEL HYBRID CATION EXCHANGE
MEMBRANES FOR REVERSE ELECTRODIALYSIS USING
SULFONATED POLY(VINYL ALCOHOL) (SPVA)/ POLY (2,6-
DIMETHYL-1,4-PHENYLENE OXIDE) (SPPO)**

A Master's Thesis
Presented to
The Academic Faculty

by

Di Jiang

In Partial Fulfillment
of the Requirements for the Degree
Master of Science in the
School of Civil & Environmental Engineering

Georgia Institute of Technology
DECEMBER 2015

COPYRIGHT © 2015 BY DI JIANG

**SYNTHESIS OF NOVEL HYBRID CATION EXCHANGE
MEMBRANES FOR REVERSE ELECTRODIALYSIS USING
SULFONATED POLY(VINYL ALCOHOL) (SPVA)/ POLY (2,6-
DIMETHYL-1,4-PHENYLENE OXIDE) (SPPO)**

Approved by:

Dr. Yongsheng Chen, Advisor
School of Civil & Environmental Engineering
Georgia Institute of Technology

Dr. Ching-hua Huang
School of Civil & Environmental Engineering
Georgia Institute of Technology

Dr. John Crittenden
School of Civil & Environmental Engineering
Georgia Institute of Technology

Date Approved: 12/03/2015

ACKNOWLEDGEMENTS

I would like to thank Dr. Yongsheng Chen for guiding me through 2014-2015. He provided me with abundant experiment opportunities and lab resources. Without his support I would never have had the chance to enter the membrane science world and improve so much through this year.

I also want to thank Dr. Hongguo Zhang, Jinji Hong, Bopeng Zhang and my other teammates in the Daniel Lab. Our RED group is the most creative and united team in Georgia Tech. They always brainstorm with me and ignite the sparks of inspiration. They help me move step by step towards my final goal. Without these teammates, as well as good friends, I would never have had accomplished goals so smoothly.

My girlfriend, Mia Lu, accompanied me, helped me acclimate to this brand new environment in U.S, and supported me with each big decision I needed to make. I'd like to thank her for her all time concern.

Finally, I feel especially thankful to my parents. It is their education and personalities that make me who I am today. Without their support, my road towards being a mature adult would encounter many more obstacles. My gratitude for their support is immeasurable, and hope they are always happy and healthy.

TABLE OF CONTENTS

	Page
ACKNOWLEDGEMENTS	iv
LIST OF TABLES	vii
LIST OF FIGURES	viii
SUMMARY	ix
<u>CHAPTER</u>	
1 INTRODUCTION	1
1.1 Technology Background	1
1.2 PRO and RED	3
1.3 Recent and ongoing research	6
2 EXPERIMENTAL	13
2.1 Materials	13
2.2 Preparation of hybrid membranes	13
2.2.1 Sulfonation of PPO	13
2.2.2 Sulfation of PVA	14
2.2.3 Membrane synthesis	14
2.3 Membrane characterization	15
2.3.1 Morphology	16
2.3.2 Chemical structure	16
2.3.3 Swelling degree	16
2.3.4 Permselectivity	17
2.3.5 Area resistance	18
2.3.6 Ion exchange capacity	19

2.3.7 RED membrane performance	20
3 RESULTS AND DISCUSSION	21
3.1 FTIR spectra study	21
3.2 Morphology of the hybrid RED membranes	22
3.3 Electrochemical properties of the hybrid RED membranes	25
3.4 SD and Area Resistance	25
3.5 Effects of sPVA loading on permselectivity and C_{fix}	27
3.6 Effects of sPVA loading on IEC	29
3.7 Effects of sPVA loading on performance potential ratio	30
3.8 RED performance of hybrid IEMs	31
4 CONCLUSION	34
APPENDIX A: Table of measured characteristics	36
REFERENCES	37

LIST OF TABLES

	Page
Table 1: Power performance of hybrid membranes and commercial CEM (FKS)	33
Table 2: Characteristics of the prepared membranes compared with a commercial membrane, FKS for RED performance	36

LIST OF FIGURES

	Page
Figure 1: Schematic representation of an RED stack	5
Figure 2: Basic chemical structure of PPO and PVA	11
Figure 3: Synthesis route of sPVA	14
Figure 4: Preparation process of the hybrid membranes	15
Figure 5: FTIR spectra of hybrid membranes	22
Figure 6: FTIR spectra of sPPO membrane	22
Figure 7: SEM surface morphology (30 μ m) of IEMs	23
Figure 8: SEM surface morphology (50 μ m) of IEMs	24
Figure 9: SEM cross-section surfaces morphology of IEMs	24
Figure 10: Area resistance and swelling degree (SD) of hybrid membranes	26
Figure 11: C_{fix} and Permselectivity of hybrid membranes	28
Figure 12: IEC of hybrid membranes	29
Figure 13: Performance potential ratio of hybrid membranes	31
Figure 14: Power density of hybrid membranes	32

SUMMARY

Ion exchange membranes (IEMs) play an important role in a reverse electrodialysis (RED) system for salinity gradient power generation. Challenges exist in the selection of appropriate membrane materials in order to reduce the capital cost of membrane manufacturing and in the design of proper RED membranes to optimize the energy-producing process. This work presents the synthesis of hybrid cation exchange membranes by incorporating two well-known inexpensive organic polymers with great film-forming ability. Sulfonated poly (2,6-dimethyl-1,4-phenylene oxide) (sPPO) polymer mixed with sulfated polyvinyl alcohol (sPVA) has been proved to have great potential as a candidate for RED membranes. The prepared membranes with 2 to 10 wt% sPVA have improved the permselectivity up to 87 % and reduced area resistance down to 1.31 ohm cm^{-2} , which is comparable to the commercially available FKS (Fumasep®, Germany) membranes. The best performance was achieved with hybrid membrane containing 5 wt% of sPVA which resulted in a gross power density at 0.46 W/m^2 . This power density is 14% greater than that achieved using commercial FKS membranes. This study shows a great potential of using organic-organic hybrid membranes for the RED power generation system.

CHAPTER 1

INTRODUCTION

1.1 Technology Background

Environmental issues including global warming, and pollution of air and water have caused severe obstacles for the development of human society. With the processes of worldwide industrialization and urbanization[1], more and more resources and energy are consumed irreversibly. The majority of the energy comes from fossil fuels, burning of which may generate greenhouse gases as well as many other pollutants. According to the International Energy Agency's Energy Technology Perspectives 2012 (IEA ETP2012) emission scenario, if human beings were to keep on today's energy consumption pattern, the world's annual energy consumption may reach 25.5 TW with a 6 degrees increase in the global temperature by 2050. This is going to change entire climate system and cause huge environmental, ecological and even economical disasters such as melting of iceberg, global climate change, new energy crisis, environmental and economical degradation, etc.[2]

Since energy consumption is a vital factor associated with many environmental problems, solving the energy problems may contribute greatly to solving above-mentioned environmental issues. Therefore, it is essential for the world to find a way to solve the energy problems. There are several methods to resolve the energy-related issues, such as changing the structure of energy industry, lowering the energy consumption, improving energy usage efficiency, and developing new energy source. However, changing the energy industry structure needs an extremely long and complicated process, not to

mention the difficulty to reduce energy consumption and keep the world's pace of development at the same time. Under the circumstance of keeping the widest use of fossil fuels in future decades, improving efficiency of energy usage is also facing huge challenges. As a result, developing cleaner and more efficient renewable energy sources becomes a feasible and promising solution.

Renewable energy takes the advantage of sustainable resources in nature. Coming from sunlight and its effects on Earth (wind, tides, etc.), most kinds of renewable energy are pollutant-free and thus show their potential for the protection of environment compared to fossil fuels. However, renewable energy accounted for only 1% of the total energy source in 2006 [3]. The development of the renewable energy is limited because of people's concerns on the engineering practicality, reliability, possibility for application, and economy and necessarily scaling for sizable power production [2]. Nevertheless, the need for cleaner energy still inspire scientists to conduct research in this area and they have studied a number of advanced technologies and made some great breakthroughs.

Currently there are several types of well-developed renewable energy options such as solar energy, wind energy, biofuel, hydro energy, tidal, and ocean wave, etc. To take advantage of solar energy, photovoltaics (PV) technology is used. Silicon batteries are needed to absorb the solar radiation and directly transfer it into electricity [2]. We can collect wind power to drive the rotation of windmill fan, and then the kinetic energy is transferred into electricity. Biofuel is another type of energy. Through heat transfer or chemical reactions, biomass is converted into energy. However, some opponents have the

view that making biofuel by biomass is not actually an environmental friendly method because the transformation processes increase the carbon footprint.

Oceans provide human beings with extraordinary amount of energy [4]. As mentioned above, hydro energy and tidal energy are all provided by the ocean. Scientists and engineers are looking for appropriate methods to harvest energy from these sources. Renewable energy can also be obtained by transferring the chemical potential between sea water and river water into electricity, which is usually referred to as salinity gradient energy [5, 6]. In 1954, R.E. Pattle et al. introduced the idea of mixing fresh and salt water to generate power.[7] Power generated by the method in this way is sometimes called “blue energy” [8]. Several advantages, like abundant, even infinite energy source (sea water, concentrated brines, etc.), non-pollutant and low cost, envisage the promising future of blue energy. According to the estimation, the annual energy generation by salinity gradient power is 2.6TW [9, 10], which is around 20% of the worldwide energy demand.

1.2 PRO and RED

There are two main technologies extracting power form salinity gradient: pressure-retarded osmosis (PRO) [11] and reverse electrodialysis (RED)[10, 12]. In a PRO system, seawater is pressurized by pump and goes into the high salinity solution chamber. Water from the low concentration chamber permeates through a semi-permeable membrane to the high salinity draw side. Through this process, power is generated by depressurizing the permeate through the hydroturbine [13]. PRO is suitable for mixing high

concentration brines[6]. National power cooperation of Norway has built the first osmosis power plant in the world (Statkraft osmotic power prototype in Hurum) and has the capacity of 4 KW. This plant uses membranes made of polyimide, which can achieve the power density of 1 W/m². However, PRO has several drawbacks: Pumping is required to provide high pressure to drive the water to the pressurized side, which requires large amount of energy; the membrane cost is high while its life cycle is relatively short.

In comparison to PRO, RED is another membrane-based technology and is suitable for power generation because of lighter membrane fouling issues and relatively high energy efficiency [14, 15]. An RED system uses ion exchange membranes (IEMs) rather than semi-permeable membranes. IEMs selectively permeate ions through the membranes and generate the chemical potential and ion flow across series of IEMs, and a set of electrodes on both ends are then used to form a circuit.

RED is the inverse of electrodialysis (ED). ED aims to apply a voltage to the system consisted of IEMs and spacers, to increase the chemical potential due to the migration of ions, and finally to desalinate the salt water. Both RED and ED systems rely on ion exchange membranes to reach their technical goals.

In an RED system, as shown in Fig.1, two different water sources, salt water and dilute water are fed into a stack. The stack is separated by several chambers. These chambers are separated by alternating series of cation exchange membranes (CEMs) and anion exchange membranes (AEMs) with spacers. Through these chambers, salt water and

dilute water are pumped alternately into each compartment, which initiates the concentration gradient across the membranes, and also generates the chemical potential through one direction. Cations go through the CEMs from concentrated side to the dilute side while anions go through the AEMs, which causes a potential gradient throughout the whole system. Two platinum electrodes are set up at two ends of the system, and electrode rinse solution is circulated through the two ends of the stack. Reduction-oxidation reactions happen at the electrodes. As a result, ion migration is transferred into electrical current, which can be harvested as electricity. [16] The stack can be composed of many connected cell pairs to fulfill large scale application.

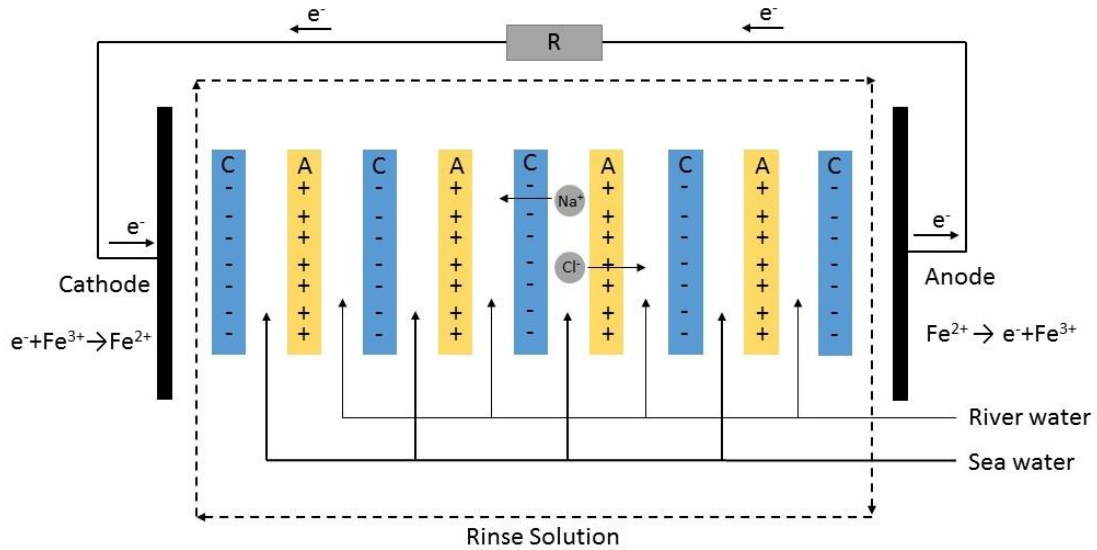


Fig.1. Schematic representation of an RED stack. C is CEM, A is AEM and R is Resistance.

Compared to conventional fossil fuel or other power productions, RED is not considered economically feasible or technically satisfied until now. As mentioned above, just like

PRO, RED's development and large scale application is strongly limited by the cost of the membranes and the performance of the membrane-based system. Optimizing the IEMs, and enhancing their performance while lowering the cost of production are crucial in this technology.

1.3 Recent and ongoing research

IEMs are the key to an RED system. Enhancing the performance of RED largely depends on the improvement of membranes. Many researchers have studied the IEMs in different areas like water treatment[17, 18], separation processes [19, 20] and power generation [21-23]. Most of these studies apply IEMs in fuel cells and electrodialysis, not specifically in RED [5]. Therefore, those membranes are not tailored for RED application, which means their major properties such as mechanical strength, chemical properties or electrochemical properties may not be optimized for RED. Even though some of these properties overlap with RED's requirement, the materials and synthesis methods still need to be tailored to maximize the performance of RED membranes.

Recently, many researchers have done RED-specific IEMs studies. They have tested different combinations of membrane materials and preparation processes, aiming to obtain the best performances using their tailor-made membranes compared to commercial IEMs. The materials and preparation processes vary among cation exchange membranes (CEMs) and anion exchange membranes (AEMs). This study focuses on CEMs, particularly on their material and synthesis procedures.

Cation exchange membranes are membranes that carry negative charge groups and can permeate positive ions while blocking the negative ions. Reversely, anion exchange membranes carry positive charge groups and can permeate negative ions while blocking the positive ions [17, 18]. People always choose polymers that have enough thermal and chemical resistance, along with great mechanical strength for thin membrane formation. At the same time, ideal material should be able to lower the production cost while maintaining or increasing electrochemical properties. For CEMs, perfluorinated material is often used for commercial application [5]. However, due to high cost, low conductivity and safety issues, perfluorinated based membranes are not widely used [5, 24]. As a result, we still need to seek alternate materials for CEMs synthesis.

Generally, all polymers with functional groups like sulfonated groups can be used as membrane materials as long as they have enough thermal and mechanical strength, or can be easily modified through low-cost processes. Hong et al. used poly (2,6-dimethyl-1,4-phenylene oxide) (PPO) as base material to fabricate CEMs and achieved great power generation performance [25]. Jeong et al. also chose PPO as polymer matrix to synthesize CEMs. Guler et al. synthesized a tailor-made CEM with polyetheretherketone (PEEK) [16]. Aesalan et al. picked polyvinyl chloride (PVC) and polystyrene as membrane base.[26] Zuo et al. selected poly(vinylidene fluoride) (PVDF) as their material for separation because of its extraordinary hydrolytic stability and film-forming properties [27]. They also introduced SiO₂ nanoparticles and blended them with organic epoxy group to enhance membranes transport performance. Lee et al. incorporated silica nanocomposite into poly (arylene ether sulfone) (PAES) to synthesize the high

conductivity, long life, and high performance membranes [21]. Other researchers focused on materials like PES, PPK[28, 29], polysulfones (PSU), poly(ether sulfone) (PES), poly(ether ketone)s (PEK), poly(phenyl quinoxaline) (PPQ), and polybenzimidazole (PBI)[30].

In order to introduce functional groups into the polymer matrix, either physical or chemical modification ought to be conducted. Usually, sulfonation and carboxylation are the two most widely-used processes for introducing the sulfonic acid group ($-\text{SO}_3^-$) and the carboxylic acid group ($-\text{COO}^-$) into the matrix.

In terms of synthesis methods for IEMs, researchers may choose different methods based on their final goal and the properties of the membrane materials. Sol-gel method is often used in organic-inorganic membranes synthesis[18]. Arsalan et al. successfully conducted membrane fabrication using sol-gel method, and synthesized PVC-based, polystyrene supported composite ion exchange membranes [26]. Mauritz et al.[31] and Khan et al. [32] also used sol-gel method to synthesize composite ion exchange membranes. Phase inversion is another common method for membrane synthesis. Jin et al. used the phase inversion method to synthesize cation exchange membranes, which has $\text{Fe}_2\text{O}_3\text{-SO}_4^{2-}/\text{sPPO}$ as the membrane base and functional groups [4]. Zuo et al.[27] used phase inversion method to form the membrane basis and then introduced the functional group to the matrix. Lee et al.[21], and Guler et al. [8] also chose phase inversion as their major synthesis method. Though sol-gel method and phase inversion method are two most important methods for IEMs synthesis, in order to satisfy the specific need for a

membrane, researchers still need to select a proper method and tailor it for specific requirements [18].

Other than the membrane synthesis research, more and more studies focus on the RED system and performance of various commercially available IEMs in an RED stack. [12, 14, 15, 33-35]. Weinstein developed a mathematic method and provided an equation to prove the feasibility of RED system in large scale [9]. According to Lacey [36], in an RED system considered economically feasible, membranes need to have the properties of low electrical resistance, long life time, high selectivity, dimensional stability and reasonable low cost. Vermass et al. found out that by reducing the membrane resistance and the stack's cell length, the gross power density of the RED system could be improved [14]. Turek et al. concluded similarly that lowering the inter-membrane distance could reduce the resistance of the system, so that the energy production of the system could be improved [37]. P. Długolecki proved that flow rate has a significant effect on the resistance of the membranes because of the influence of diffusion boundary layer.[38] Alexandros Daniilidis et al. generated a model to study the financial feasibility of the RED and pointed out two performance indicators, unit area power output (W/m^2) and energy efficiency (%). According to their model, prices as well as membrane performance are the key factors for large scale application of RED. The price of the membrane should be much lower than the current number in order to be competitive [39].

There are also some studies combining RED with other similar membrane technologies. Forgacs took ED as the reference, and built a model for RED's power generation. Li

Weiye et al. created a novel method to combine the processes of RED and reverse osmosis (RO) to an integrate system. This system improved both the performance of traditional RO system and the efficiency of RED [40].

Several researchers pointed out that low resistance, high fixed-charge density, high transport number and a considerable permselectivity are essential for ion exchanging process [33, 41-43]. Since studies on RED specific membranes are limited, it is really challenging to tailor the membranes for features significant to RED [44, 45]. Therefore, it is important to choose an appropriate membrane material that has the potential to meet RED's requirements.

PPO is a very common engineering thermoplastic that consists of an aromatic ring, a phenol group and two methyl side groups at position 2, 6 of the ring (Fig. 2(a)). PPO is considered an ideal polymer for membrane formation because of its great membrane-forming ability, high physical strength, great chemical and thermal stability, low cost and high glass transition temperature [18, 46-49]. According to PPO's chemical structure, its aromatic ring is susceptible to simple polymer modification [50, 51], and its methyl group can also be functionalized by capping, coupling, etc. However, PPO has its own limitations due to its hydrophobic property and lack of charged functional groups. This means it is hard to dissolve into dipolar solvents and it lacks ionized groups that are essential in IEMs. To fix these drawbacks, one alternative is to introduce functional groups into the polymer matrix. Through reactions of sulfonate agents like chlorosulfonic acid with PPO, sulfonate groups ($-\text{SO}_3^-$) are introduced to the polymer chain, and

therefore forms sulfonated poly 2,6-dimethyl-1,4-phenylene oxide (sPPO). sPPO has both hydrophilic and charged functional groups and therefore shows great electrochemical potential. sPPO is widely used in industrial processes [46, 52] like gas separation and fuel cells, etc.[51].

However, sPPO is still not an ideal material due to its limitation in aqueous separation as it is found highly erodible in the organic solvents [53]. One possible solution is to blend sPPO with other inorganic or organic materials[54]. Inorganic materials can be nanocomposites like SiO₂ or Fe₂O₃ nanoparticles, and as previously mentioned, sol-gel processes are commonly used to form this kind of organic-inorganic membrane. Organic materials are polymers with great stability and electrochemical properties in organic solvents. Polyvinyl alcohol (PVA) is such a kind of material.

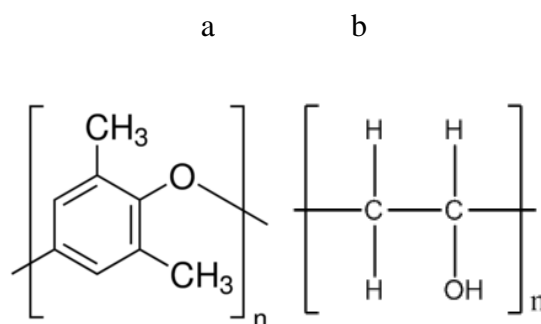


Fig.2. Basic chemical structure of a) PPO and b) PVA

PVA is a cheap, odorless and non-toxic, and biodegradable polyhydroxy polymer [55-57]. It is considered as a relatively clean polymer material because it is easy to prepare (both water-soluble and organic solvent-soluble). Another advantage of PVA is that the

hydroxyl groups in PVA (Fig.2 (b)) contribute to PVA's highly hydrophilic property and may offer cross-linking with other polymers [58, 59]. Besides, PVA has great chemical-resistance and ductility for membrane formation [56, 60-65].

However, similar to PPO, PVA is a neutral material that lacks charged groups for ion exchange. In order to improve its electrochemical conductivity, further modification is needed. For CEMs application, similar process of sPPO modification is used: Sulfonated groups are introduced into PVA. After sulfating with sulfuric acid or sulfosuccinic acid, the new formed sPVA will become negative charged and will exhibit significantly improved conductivity [66, 67].

Since sPVA can provide both charged groups and extra hydrophilicity, it is reasonable to blend sPVA with sPPO to synthesize a new kind of IEMs. Therefore this study focuses on the hybrid membranes made of poly (2,6-dimethyl-1,4-phenylene oxide) (PPO) and polyvinyl alcohol (PVA). As no specific research has been made on sPPO-sPVA membranes in an RED system, this research offers a design strategy for this new type of RED-specific membranes. This study also presents our investigation into sPVA loading's effect on membrane performance.

CHAPTER 2

EXPERIMENTAL

2.1 Materials

PPO (Sigma-Aldrich, analytical standard, M_w 30,000, M_n 20,000) was used as base polymer. Chloroform (anhydrous, 99%) purchased from Sigma-Aldrich was used as a solvent for sulfonating PPO. Dimethylsulfoxide (DMSO) (ACS grade, 99.9%) was obtained from VMR and used as another solvent for membrane synthesis. Chlorosulfonic acid (Sigma-Aldrich, 99%), methanol (Sigma-Aldrich, 99%) are used for PPO sulfonation. Sulfuric acid (Sigma-Aldrich, 98%) and Ethyl alcohol (Sigma-Aldrich, 99%) were used for PVA sulfating. Poly (vinyl alcohol) (Sigma-Aldrich, M_w 146,000-186,000, 99+% hydrolyzed) was used as received.

2.2 Preparation of hybrid membranes

2.2.1 Sulfonation of PPO

The process of sulfonating PPO is similar to existing paper[25]. 6 wt% PPO (4.9g in 50 ml) powder was dissolved in chloroform by magnetic mixing under room temperature for 20 min. 9 vol% (5ml in 50ml) chlorosulfonic acid-chloroform solution was slowly added to PPO solution at the speed of 1 plastic head dropper every 1-2 minutes under continuously stirring. Sulfonated PPO precipitation, the brown flocs, started to form. The precipitations were washed by DI water multiply times under stirring until neutral pH was achieved. The solids were then collected and dissolved into methanol. After complete mixing, the solution was poured to a flat bottom glass tray and was dried under

ambient condition for over 24 hours. The transparent brown particles, sPPO, were then collected after complete drying.

2.2.2 Sulfation of PVA

Required PVA was dissolved into DI water at the weight ratio of no more than 1:4. After PVA was completely dissolved, excessive concentrated sulfuric acid (H_2SO_4 , 98%) was slowly added into the PVA-water solution. Then the PVA solution was stirring at 40°C in water bath. After at least 4 hours, ethyl alcohol was added, and white precipitations, sPVA, were formed (Fig.3). The solids were washed by ethyl alcohol to neutral pH and dried in vacuum oven for at least 24 hours at 50°C .

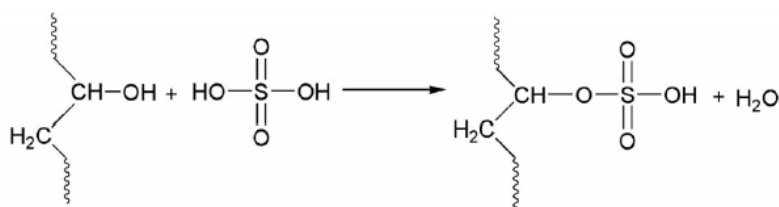


Fig. 3. Synthesis route of sPVA

2.2.3 Membrane synthesis

Hybrid RED membranes were prepared by solvent evaporation method. sPPO polymer was dissolved in DMSO at the weight ratio of 1:4 as solution 1. sPVA was dissolved in DMSO at 0%, 2%, 5%, 10%, 15% and 20% weight percentage (total weight related to sPPO weight) as solution 2. These two solutions were then mixed and stirred at 40°C for over 48 hours (Fig 4). Afterwards, the mixed solution was vibrated in ultrasonic bath for at least 30 minutes in order to get sPVA uniformly dispersed. The resulting light yellow

solution was then cast onto a glass plate by a doctor blade. The blade was adjusted to achieve a 100 μm wet thickness of the membrane. Then the membrane was dried in a vacuum oven at near 50°C for 24 hours and then 60°C for 6 hours to remove the solvents entirely. After that process, the membrane was manually peeled off from the plate by rinsing it into warm water. Lastly, the membrane was soaked in 1M hydrochloride acid solution for one day and stored in 0.5M NaCl solution.

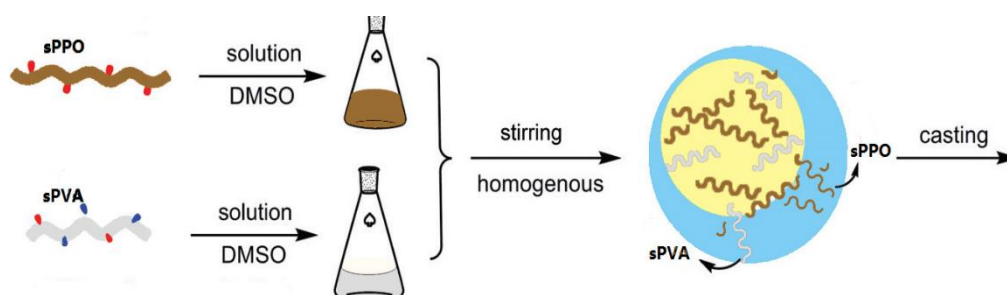


Fig. 4. Preparation process of the hybrid membranes

2.3 Membrane Characterization

The IEMs have different kinds of physical properties and electrochemical properties.[16] Physical properties include morphology, thickness and swelling degree. Electrochemical properties include permselectivity, area resistance and ion exchange capacity. Lots of studies tried to explain how membranes properties influence the performance of RED system. However, the dominant property related to RED system's performance remains unknown [16]. These properties can either be characterized by experimental methods or calculations. As previously mentioned, different applications may target at different membrane properties. For RED, since its target is to generate power rather than doing separation or filtration, electrochemical properties optimization of product membrane

should be this study's first priority and the characterizations of electrochemical properties are therefore of great importance.

2.3.1 Morphology

The membrane morphology includes its thickness and surface characteristics. In this study, morphology was analyzed by scanning electron microscopy (SEM) (Zeiss Ultra60 FE-SEM), including both cross-section observation and surface area observation.

Samples were washed up by DI water and dried over night before doing tests. For cross-section observation, the sample was pre-treated by nitrogen liquid and was manually cut to get an original cross-section area.

2.3.2 Chemical Structure

The chemical structure of the membrane means all chemical bindings. This was studied through Fourier transform infrared (FTIR) Spectrometer (Digilab FTS7000) along with a microscope (Digilab UMA 600). The spectrum was obtained with 32 scans per sample at a 4 cm^{-1} resolution. The range of the spectrum was $4000 - 700\text{ cm}^{-1}$.

2.3.3 Swelling degree

Swelling degree (SD), also called water uptake, is a property showing the water content of the membrane under given conditions. SD is dependent on the membrane material, structure and solution conditions [43, 68]. SD can be reduced through the increasing cross-linking degree [4, 69]. Besides, swelling degree is also related to other membrane properties like permselectivity and resistance [33] because the process of the swelling can

be regarded as the dilution of functional groups in membrane. Thus, SD is an important indicator of membrane performance.

In this study, dry weight and wet weight of the membrane were measured to calculate the SD by the following equation[70]:

$$SD = \frac{W_{wet} - W_{dry}}{W_{dry}} \times 100\% \quad (1)$$

where W_{wet} is the wet weight, W_{dry} is the dry weight of the membrane.

2.3.4 Permselectivity

Permselectivity defines selecting ability of IEMs. It is decided by the type and number of functional groups in the membrane. Theoretically, the permselectivity should be 1, which means the IEMs will completely reject the co-ions from passing through themselves.

However, the value is always below 1 because some co-ions will permeate and contribute to the ion transport [71]. Permselectivity is vital because it decides the maximum chemical potential of the membrane.

In this research, permselectivity was characterized by a static potential measurement test. The test equipment consists of two separated cells. Tested membrane was placed at the connection of two cells with effective area of 4.8 cm^2 . Sodium chloride solutions of 0.1M and 0.5M concentrations flew into the two separated cells respectively, and created potential through the membrane. The potential was measured by a multimeter (Tektronix, US) with Ag/AgCl reference electrodes (Hanna Instruments, US) [25]. The permselectivity is then calculated by following equation:

$$\alpha(\%) = \frac{\Delta V_{measured}}{\Delta V_{theoretical}} \times 100 \quad (2)$$

where α is the membrane permselectivity (%), $\Delta V_{measured}$ is the measured membrane potential value (V) and $\Delta V_{theoretical}$ is the theoretical membrane potential, 0.0379 V, which can be calculated by Nernst Equation. [72].

2.3.5 Area resistance

Area resistance is the internal resistance that inhibits the ions and electrons from migrating. The resistance of a membrane is affected by many factors in a membrane process, like the ion transport or the IEC of a membrane. Even the temperature may have a negative effect on the resistance: the resistance may decrease when temperature rises [72]. A whole RED system is very similar to a battery, thus the area resistance is just like resistance in a circuit. Since RED system targets to generate more power, it is necessary to keep the resistance as low as possible to gain enough potential and to reduce energy loss.

Like permselectivity measurement, the area resistance was also measured by above two-cell device. These two cells were both filled with 0.5 M NaCl solution and were separated by a 0.38 cm² IEM. Since the resistance depends on the temperature, the measurement was conducted under the room temperature. We used two titanium electrodes coated with Ru-Ir oxides and a potentiostat (Vertex, Ivium Technology) to measure the resistance by impedance spectroscopy (IS) [25, 73]. The frequency range was from 10-10⁵ Hz with an oscillating voltage of 0.1V amplitude

2.3.6 Ion exchange capacity

The ion exchange capacity reflects the number of fixed charges in the membrane. Fixed charges number is related to functional groups, which is ($-\text{SO}_3^-$) in this study. Higher IEC means more ion exchange groups in the membrane, and thus better performance.

IEC was measured by the titration method [25]. Dry membranes were weighed and then immersed in 1.0 mol/L HCl solution for 15 hours for converting to H^+ form. Excessive HCl was then rinsed off by DI water. After that the membranes were immersed into 1M NaCl solution for 6 hours. The solution was then titrated with 0.01 M NaOH solution using phenolphthalein as indicator. The IEC then was determined by the following equation:

$$IEC = \frac{C_{NaOH} \times V_{NaOH}}{W_{dry}} \quad (3)$$

where C_{NaOH} is NaOH solution concentration (mol/L), V_{NaOH} is the volume of NaOH solution (L) used for titration. W_{dry} is the dry weight of the membrane (g).

As mentioned above, a high swelling degree means more dilute charged groups, so SD is a negative factor in membrane performance. Inversely, high IEC often means high density of charged groups, which is a positive factor. By using the equation of IEC over SD, the fixed charge density (also called fixed charge concentration) is defined to represent the comprehensive effects of IEC and SD on membrane electrochemical properties [74]:

$$C_{fix} = \frac{IEC}{SD} \quad (3)$$

2.3.7 RED membranes performance

An RED stack was used to test the power density of the membranes. As shown in Fig.1, the whole stack consists of two electrodes, 5 CEMs (FKS (Fumasep®, Germany) or synthesized membranes) and 4 AEMs (FAS)(Fumasep®, Germany) with the effective area of 4 cm×9 cm. These CEMs and AEMs were arranged at intervals and separated by spacers between two endplates. Simulated salt water (0.5M NaCl) and river water (0.017 M NaCl) were fed into the stack alternatively [25]. Rinse solution at the two sides consists of NaCl (0.25 M), $K_4Fe(CN)_6$ (0.05 M) and $K_3Fe(CN)_6$ (0.05 M). Woven fabric spacers at the thickness of 250 μ m function as separating membranes and determining the distance of water flow for seawater and river water. Two silver wires placed half into the stack between electrodes and endplates were used as cathode and anode. Potentionstat in the galvanostatic mode was used to record the potential and current (E-I) data for calculating the gross power generation. Peristaltic pumps (Masterflex, Cole-Parmer) were used to control the flow rate through the RED system.

CHAPTER 3

RESULTS AND DISCUSSION

3.1 FTIR spectra study

FTIR spectra tests were conducted on sPVA-sPPO membrane samples with different weight percentage. The results of FTIR spectra are shown in Fig. 5 and Fig. 6. The broad bands showing between 3200 and 3600 cm^{-1} indicate the stretching vibrations of $-\text{OH}$ groups. The peaks at 942 cm^{-1} , 1644 cm^{-1} and 2856 cm^{-1} represent the stretch of C-O-C groups, CH- groups and $-\text{CH}_2-$ groups [16], and the peak of 1465 and 1599 cm^{-1} represents the aromatic groups. All of the above bands are from the original PPO polymer. The evidence of $-\text{SO}_3\text{H}$ substitution to PPO aromatic rings can be seen at the peak of 1060 cm^{-1} , which means the reaction of sulfonation. Vibration bands of C-S-O stretching were seen at 1186 cm^{-1} . FTIR peak at 3389 cm^{-1} is formed from stretch vibration absorption shifted from hydroxyl of sPVA absorption (3434 cm^{-1}), which is caused by $-\text{OH}$ and $-\text{SO}_3\text{H}$'s hydrogen reactions. Overall, the FTIR results revealed the successful sulfonation of the PPO and sulfation of PVA polymer.

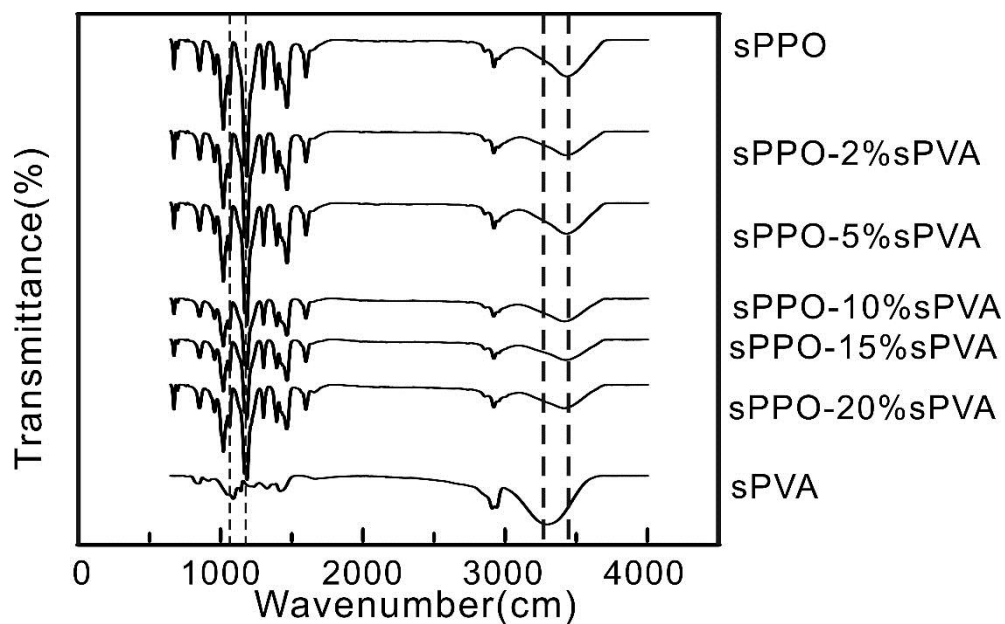


Fig. 5. FTIR spectra of hybrid membranes

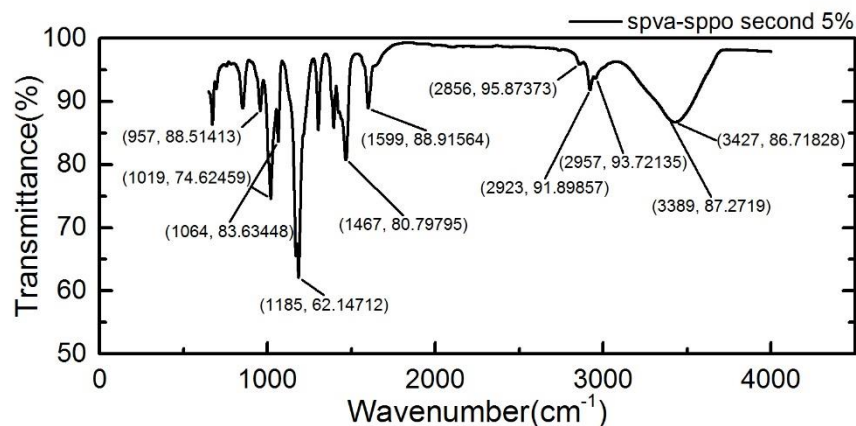


Fig. 6. FTIR spectra of sPPO membrane

3.2 Morphology of the hybrid RED membranes

In order to observe the structures and surface differences in sPVA-sPPO membranes with different sPVA ratios, SEM was used to study the membrane morphology (Fig.7, Fig.8 and Fig.9). Both top surfaces and the cross-section areas were analyzed.

In Fig. 7, 8, and 9, SEM images of both (b) sPPO-2% sPVA and (c) sPPO-5% sPVA showed uniform distribution with comparatively smaller pores through the entire polymer matrix, both on their top surfaces and cross sections. However, when membrane samples' sPVA weight ratio went above 5%, like (d) sPPO-10% sPVA, (e) sPPO-15% sPVA, and (f) sPPO-20% sPVA in Fig. 7, 8, and 9, their pore size distributions were less uniform and pore sizes became much larger. According to the cross-section images, the thickness of the membranes remained same in the range of near 30-50 μm despite of the sPVA ratio change in these membranes. Meanwhile, the cross-section surfaces were dense in structure. When the content of sPVA increased, the membranes' degree of compaction decreased sharply (Fig.9).

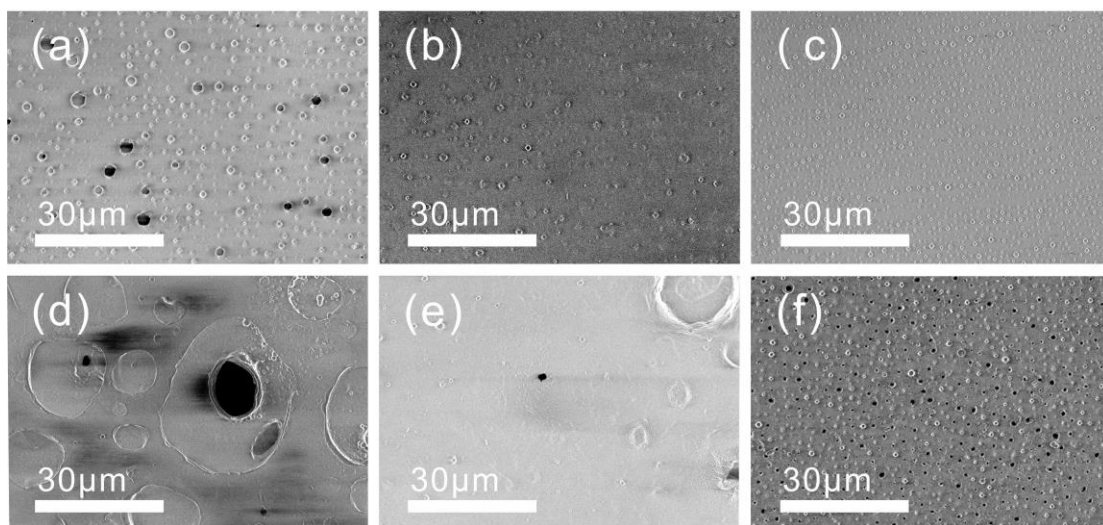


Fig. 7. SEM surface morphology (30 μm) of (a) sPPO, (b) sPPO-2% sPVA, (c) sPPO-5% sPVA, (d) sPPO-10% sPVA, (e) sPPO-15% sPVA, (f) sPPO-20% sPVA;

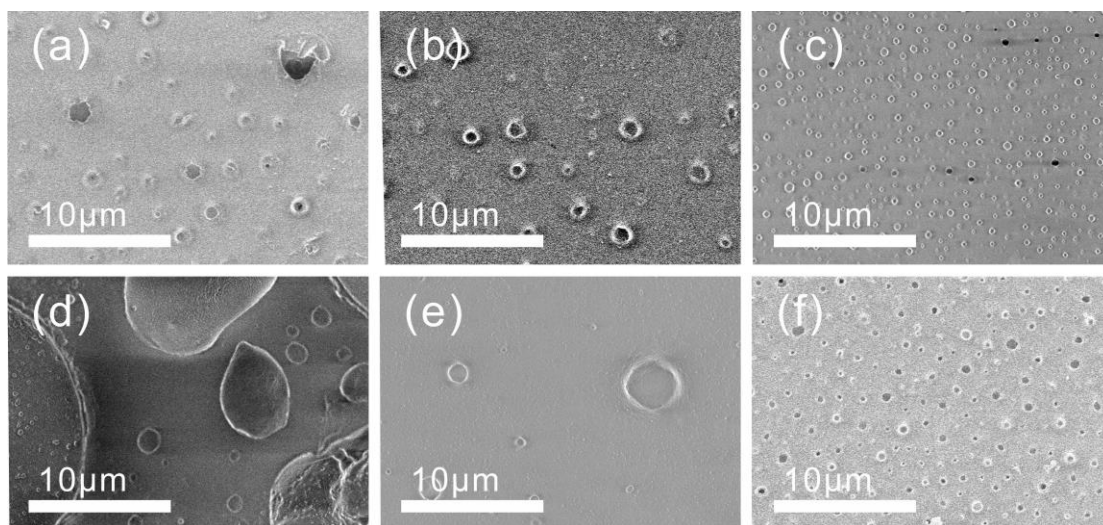


Fig. 8. SEM surface morphology (10 μ m) of (a) sPPO, (b) sPPO-2% sPVA, (c) sPPO-5% sPVA, (d) sPPO-10% sPVA, (e) sPPO-15% sPVA, (f) sPPO-20% sPVA

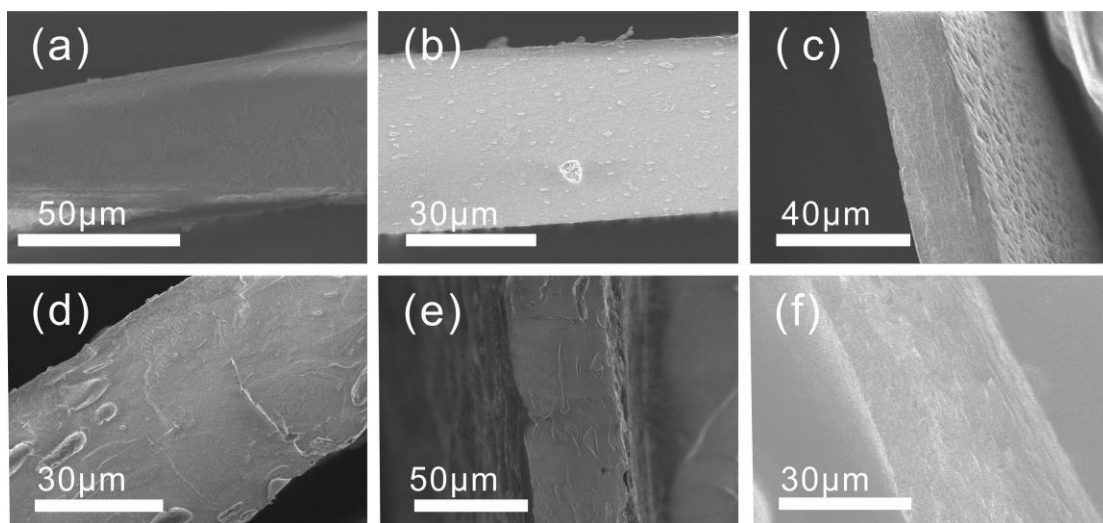


Fig. 9. SEM cross-section surfaces morphology of (a) sPPO, (b) sPPO-2% sPVA, (c) sPPO-5% sPVA, (d) sPPO-10% sPVA, (e) sPPO-15% sPVA, (f) sPPO-20% sPVA

3.3 Electrochemical properties of the hybrid RED membranes

In this study, several key electrochemical properties of the synthesized hybrid membranes including permselectivity, IEC, SD, area resistance and fixed charge concentration were measured for evaluating their power generation performance in a small scale RED system. Additionally, the value of the square of permselectivity (P) over area resistance (R) is also defined as the performance potential ratio [25] in order to explore the comprehensive influence of P and R to membrane performance. In this study, all values were measured three times to ensure the data reliability and the error bars are in all case no more than 5%. As reference, the corresponding data of commercial membranes, FKS (Fumasep®, Germany) were also listed in Table 2 of Appendix A.

3.4 SD and Area Resistance

As mentioned previously, SD represents the water uptake of the membrane. The value of SD depends on membrane material and structure. Therefore, in this study, the SD values differed when the content of sPVA changed. The SD increased from 45.63% to 93.91% when content of sPVA increased (Fig. 10), which means higher hydrophilicity. The increased hydrophilicity is mainly attributed to a reduced cross-linking degree. Increasing SD is usually helpful for reducing the area resistance of a membrane [16, 49, 72, 75]. Similar trend could be seen in Fig.10.

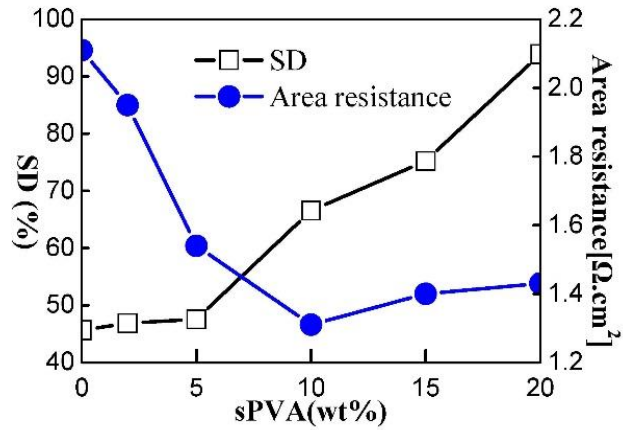


Fig. 10. Area resistance and swelling degree (SD) of hybrid membranes

As is showed in Fig.10, when the content of sPVA increased, the area resistance of the membranes decreased dramatically from $2.11 \text{ ohm}\cdot\text{cm}^2$ (0 wt% sPVA) to $1.31 \text{ ohm}\cdot\text{cm}^2$ (10 wt% sPVA). However, when sPVA content kept increasing, the resistance revealed a slight increase, from 1.31 to $1.43 \text{ ohm}\cdot\text{cm}^2$ (20 wt% sPVA). One possible explanation for this phenomenon is that factors controlling the resistance are complicated. SD, together with charge density, polymer matrix density and the surface morphology may all contribute to the increase/decrease of the resistance. Therefore, it is impossible to draw a single linear connection between one or more these factors and resistance. Another research pointed out that the pore formation and surface roughness of the composite will affect the transport of ions, permselectivity and also conductivity [19]. In this study, when SD rose, other factors might start taking dominant influence on the resistance, and formed the trend of resistance in Fig.10. Above all, the lowest area resistance was achieved at $1.31 \text{ ohm}\cdot\text{cm}^2$ when the membrane contained 10 wt% of sPVA.

3.5 Effects of sPVA loading on permselectivity and C_{fix}

The permselectivity of the hybrid membranes describes the ability of membranes' cations selectivity from a solution containing both cations and anions, which is determined by the type of the fixed charges [76, 77]. In general, membranes with a lower fixed charge density have a lower selectivity as well [33]. Permselectivity of mobile cations through the membranes is also often affected by the electrolyte solutions' concentration differences.

As is shown in Fig.11, the membrane permselectivity and C_{fix} have relatively clear relationships with the loading of sPVA. When the loading of sPVA increased from 0% to 20%, the clear drop of C_{fix} could be observed, from 4.54 (0 wt% sPVA) to 1.68 (20 wt% sPVA). This is because with the increase of sPVA content, the swelling property of the membranes was greatly enhanced, which led to increase of distance between the ion exchange groups, then reduce of the fixed-charge density[33].

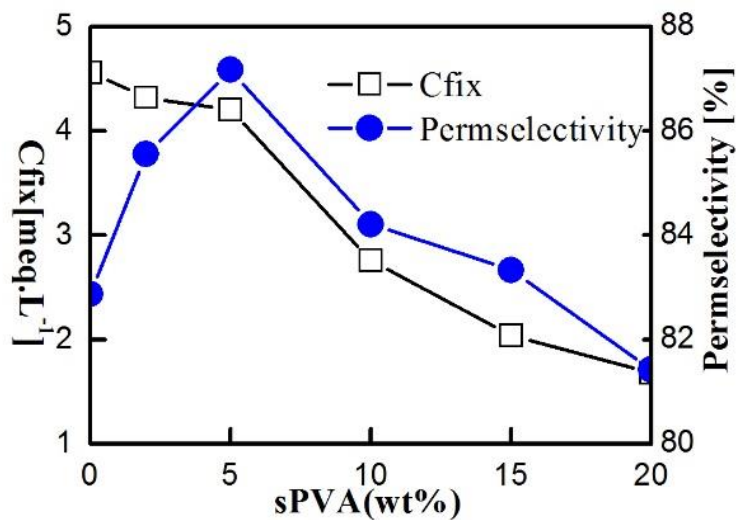


Fig. 11. C_{fix} and Permselectivity of hybrid membranes

The permselectivity showed the similar trend as C_{fix} changed. However, when sPVA loading varied from 0% to 5%, the permselectivity increased while C_{fix} decreased. The reason is that even though charge density has great influence on permselectivity, there is no straightforward relationship between these two characters. Therefore, like the relationship between SD and resistance, other factors such as density of polymer matrix, and hydrophilicity, etc. need to be considered. A more comprehensive understanding of these properties is required since these factors are all inner-related. In this study, the highest membrane permselectivity was achieved when the loading of sPVA reached 5 wt% (Fig. 11).

3.6 Effects of sPVA loading on IEC

For the membranes prepared with hydrophobic materials like PPO in this study, when sPVA loading increased, the SD values increased, and IEC decreased (Fig. 12). As mentioned above, when SD increased, the membrane swelled, so the density of functional groups dropped and diluted the charged groups, which led to low IEC value. Low IEC caused low membrane ion conductivity, and therefore decrease the transport ability. As a result, excessive sPVA loadings will decrease the IEC and weaken ion exchange properties, which will directly lead to lower membrane performance.

For FKS commercial membranes, having high IEC does not necessarily result in low area resistance. In our experiments, both the IEC and resistance had decreasing trends when sPVA loading increased (Fig.10 and Fig.12). However, there's no pronounced conclusion that IEC and resistance are always correlated [33, 78].

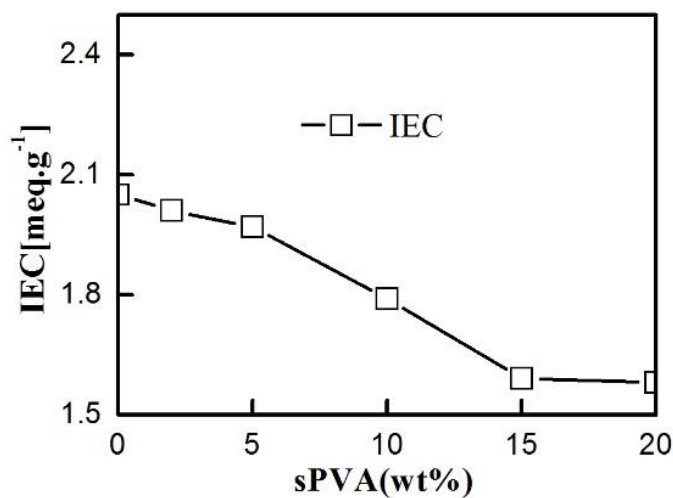


Fig. 12. IEC of hybrid membranes

3.7 Effects of sPVA loading on performance potential ratio

There are some existed studies on mathematical relationships between different membrane properties and membrane performance. According to Kirchhoff's law, theoretical maximum membrane stack power output (P_{\max}) can be calculated through the following equation:

$$P_{\max} = \frac{[\alpha RT / F \ln(\alpha_c / \alpha_d)]^2}{AR_{\text{stack}}} \quad (5)$$

where R is gas constant ($8.314 \text{ Jmol}^{-1}\text{K}^{-1}$), T is absolute temperature (K), F is Faraday constant (96485 Cmol^{-1}), α is average apparent permselectivity of the membrane (%), α_c is activity (molL^{-1}) of the sea water solution, α_d is the activity (molL^{-1}) of river water solution, A is the membrane area (m^2), and R_{stack} is stack resistance. The equation is based on the hypothesis that RED system can generate a maximum power under the state that R_{stack} is equal to the load resistance of the system [9, 79].

P_{\max} equation also predicts the relationship among individual membrane properties, which can be used to compare the membrane performances in the RED system with different kinds of membranes [5, 9, 14, 72].

According to P_{\max} equation, it is clear that permselectivity and resistance are two key factors for power generation. Thus, P^2/R can be used as an indicator of the power performance. In this study, loading from 5-15% sPVA achieved the highest P^2/R value, then this value decreased when sPVA loading increased (Fig. 13). This result indicates that the maximum power density level will show in the range of 5% - 15% sPVA.

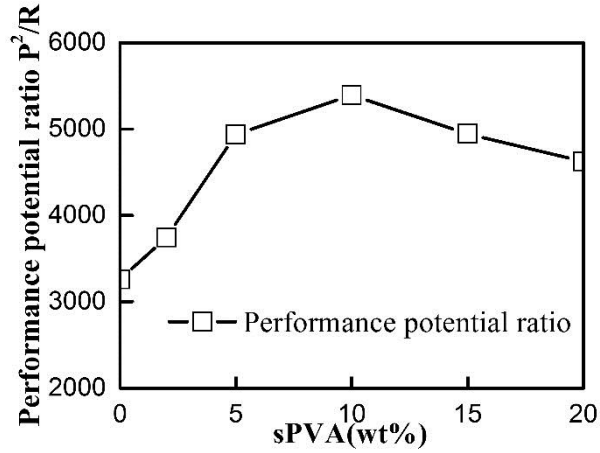


Fig. 13. Performance potential ratio of hybrid membranes

What still needs to be clarified is that, without considering other constants, which membrane property has the dominant influence on RED system performance is not yet fully known, and the relationships between these properties are not clearly understood.

3.8 RED performance of hybrid IEMs

Power density of the membranes were tested by the RED stack mentioned in Chapter 2. Five commercial CEMs, FKS (Fumasep®, Germany, thickness of 50 μ m) and AEM, FAS (Fumasep®, Germany, thickness of 50 μ m) were tested in the stack under the flow rate of 0.8 cm/s as a reference. Under the same condition, FKSS were replaced by synthesized sPPO-sPVA membranes to exam RED performance. Then the gross power density was estimated by E-I curve obtained by the Potentionstat.

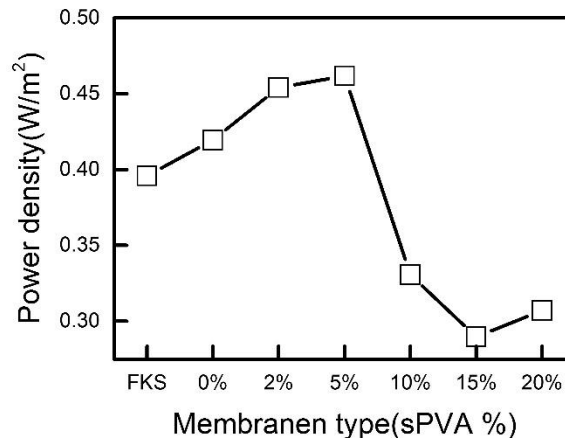


Fig.14. Power density of hybrid membranes

As can be seen in Fig.14, when the loading of sPVA in membrane increased, the gross power density increased from 0.42 W/m² (0 wt% sPVA) to 0.46 W/m² (5 wt% sPVA). However, when sPVA loading continued to increase from 5% to 10%, power density of the membrane had a great decrease to 0.35 W/m². Compared to commercial FKS membranes, membranes with sPVA loading between 0% and 5% achieved higher density, and 5% sPVA membranes reached the peak performance of 0.462 W/m², 14% higher than commercial ones. The test result showed that these hybrid tailored membranes have greater potential in power generation than commercial IEMs. They not only achieved higher power density, but also superior in low cost of materials as well as extremely easy and nontoxic membrane forming processes. The relatively high permselectivity of 87.17%, low area resistance of 1.54 $\text{ohm}\cdot\text{cm}^2$ played an important role in determining the power output. The membrane with sPVA loading of 15% had the worst performance, which means moderate loading of hydrophilic sPVA will help improve membrane performance, but excessive loading may have a negative effect. As mentioned above, the loading of sPVA will inevitably affect the polymer matrix and its electrochemical

properties, so as to influence its power density. Although changes in these properties (morphology, IEC, area resistance, permselectivity and SD) agree well with change in power density, the relationships between these properties and power generation performance are still unclear. A more reliable interpretation or model on the hybrid membrane needs to be deduced based on more extensive research. This current design of organic-organic RED-tailored membranes, however, is still a great progress, pointing out a new direction to synthesize RED membranes.

Table 1. Power performance of hybrid membranes and commercial CEM (FKS)

Membranes (PVA wt%)	Gross Power Density(W/m ²)
0	0.420
2%	0.451
5%	0.462
10%	0.331
15%	0.290
20%	0.307
FKS	0.396

CHAPTER 4

CONCLUSION

This research focused on the membrane synthesis and aimed to find a simple method to synthesize a new type of CEMs that has better or comparative performance as commercial membranes. Therefore its characteristics for power generation performance in the RED system were investigated. Based on the experiments, conclusions are as follows:

1. A new type of hybrid organic-organic cation exchange membranes was successfully synthesized by solvent evaporation method. Its physical, electrochemical properties were investigated. This kind of membrane was also tested in an RED stack for its power generation performance study.
2. By incorporating small amount of sulfated PVA (sPVA) into sPPO polymer, IEMs' properties were considerably improved. Different loadings of sPVA were studied to optimize the membrane performance in the RED stack. For sPVA loading ranging from 0% to 20%, membrane properties IEC, SD, area resistance and permselectivity were tested. By controlling the sPVA loading, the hybrid membrane was found to be optimized at the concentration of 5 wt% sPVA for power generation. Compared to commercial CEMs, FKS membranes, the performance of 5 wt% sPVA membranes improved 14% in power output, proving their great potential for commercialized RED use.

3. Compared to FKS membranes, the newly synthesized membrane in this study also superior in much cheaper and nontoxic materials, which may significantly reduce the production cost. In terms of the synthesis processes, membranes in this study were synthesized by simple film-forming processes without complicated procedures or toxic chemicals, indicating great economical and scale-up potential.
4. This study also suggested some possible correlations between all kinds of membrane physical, electrochemical properties and the power outputs. Performance potential ratio, fixed-charged density, etc. could all be used as indicators of membrane performance. However, the precise relationships between these key membrane properties with power density and the effect of hybrid organic membrane on RED are still unknown, which requires further study. Most importantly, the studies towards RED-tailored IEMs are extremely limited. Further studies are needed for more sophisticated theory of membrane synthesis.

APPENDIX A

TABLE OF MEASURED CHARACTERISTICS

Table 2. Characteristics of the prepared membranes compared with a commercial membrane, FKS for RED performance.

Membrane (wt% of PVA)	P [%]	Area resistance [Ωcm^2]	Performance potential ratio P^2/R	IEC [meq.g^{-1}]	SD (%)	C_{fix} [meq.L^{-1}]
0	82.87	2.11	3259.75	2.05	45.63	4.56
2%	85.55	1.95	3744.90	2.01	46.85	4.32
5%	87.17	1.54	4939.50	1.97	47.55	4.2
10%	84.21	1.31	5393.72	1.79	66.53	2.76
15%	83.33	1.40	4944.61	1.59	75.22	2.04
20%	81.42	1.43	4625.67	1.58	93.91	1.68
FKS	96.00	1.87	4928.34	1.40	22	6.36

REFERENCES

- [1] R.E. Dunlap, A.K. Jorgenson, Environmental Problems, in: The Wiley-Blackwell Encyclopedia of Globalization, John Wiley & Sons, Ltd, 2012.
- [2] I. Dincer, Renewable energy and sustainable development: a crucial review, Renewable and Sustainable Energy Reviews, 4 (2000) 157-175.
- [3] J.A. Fay, D.S. Golomb, Energy and the environment: Scientific and technological principles, 2nd edition, Environmental Progress & Sustainable Energy, 31 (2012) 9-9.
- [4] J. Gi Hong, Y. Chen, Evaluation of electrochemical properties and reverse electrodialysis performance for porous cation exchange membranes with sulfate-functionalized iron oxide, Journal of Membrane Science, 473 (2015) 210-217.
- [5] J.G. Hong, B. Zhang, S. Glabman, N. Uzal, X. Dou, H. Zhang, X. Wei, Y. Chen, Potential ion exchange membranes and system performance in reverse electrodialysis for power generation: A review, Journal of Membrane Science, 486 (2015) 71-88.
- [6] J.W. Post, J. Veerman, H.V.M. Hamelers, G.J.W. Euverink, S.J. Metz, K. Nijmeijer, C.J.N. Buisman, Salinity-gradient power: Evaluation of pressure-retarded osmosis and reverse electrodialysis, Journal of Membrane Science, 288 (2007) 218-230.
- [7] R.E. Pattle, Production of Electric Power by mixing Fresh and Salt Water in the Hydroelectric Pile, Nature, 174 (1954) 660-660.
- [8] E. Guler, Y. Zhang, M. Saakes, K. Nijmeijer, Tailor-Made Anion-Exchange Membranes for Salinity Gradient Power Generation Using Reverse Electrodialysis, ChemSusChem, 5 (2012) 2262-2270.
- [9] J.N. WEINSTEIN, F.B. LEITZ, Electric Power from Differences in Salinity: The Dialytic Battery, Science, 191 (1976) 557-559.
- [10] G.Z. Ramon, B.J. Feinberg, E.M.V. Hoek, Membrane-based production of salinity-gradient power, Energy & Environmental Science, 4 (2011) 4423-4434.
- [11] K. Lee, R. Baker, H. Lonsdale, Membranes for power generation by pressure-retarded osmosis, Journal of Membrane Science, 8 (1981) 141-171.
- [12] P. Długotański, A. Gambier, K. Nijmeijer, M. Wessling, Practical potential of reverse electrodialysis as process for sustainable energy generation, Environmental science & technology, 43 (2009) 6888-6894.
- [13] S. Loeb, Large-scale power production by pressure-retarded osmosis, using river

water and sea water passing through spiral modules, *Desalination*, 143 (2002) 115-122.

[14] D.A. Vermaas, M. Saakes, K. Nijmeijer, Doubled power density from salinity gradients at reduced intermembrane distance, *Environmental science & technology*, 45 (2011) 7089-7095.

[15] J.W. Post, H.V. Hamelers, C.J. Buisman, Energy recovery from controlled mixing salt and fresh water with a reverse electrodialysis system, *Environmental science & technology*, 42 (2008) 5785-5790.

[16] E. Güler, R. Elizen, D.A. Vermaas, M. Saakes, K. Nijmeijer, Performance-determining membrane properties in reverse electrodialysis, *Journal of membrane science*, 446 (2013) 266-276.

[17] T. Sata, *Ion Exchange Membranes: Preparation, Characterization, Modification and Application*, The Royal Society of Chemistry, 2004.

[18] T. Xu, Ion exchange membranes: State of their development and perspective, *Journal of Membrane Science*, 263 (2005) 1-29.

[19] J.-H. Choi, S.-H. Kim, S.-H. Moon, Recovery of lactic acid from sodium lactate by ion substitution using ion-exchange membrane, *Separation and purification technology*, 28 (2002) 69-79.

[20] C. Klaysom, S.-H. Moon, B.P. Ladewig, G.M. Lu, L. Wang, The influence of inorganic filler particle size on composite ion-exchange membranes for desalination, *The Journal of Physical Chemistry C*, 115 (2011) 15124-15132.

[21] C.H. Lee, K.A. Min, H.B. Park, Y.T. Hong, B.O. Jung, Y.M. Lee, Sulfonated poly (arylene ether sulfone)–silica nanocomposite membrane for direct methanol fuel cell (DMFC), *Journal of Membrane Science*, 303 (2007) 258-266.

[22] D.-W. Seo, Y.-D. Lim, S.-H. Lee, Y.-G. Jeong, T.-W. Hong, W.-G. Kim, Preparation and characterization of sulfonated amine-poly(ether sulfone)s for proton exchange membrane fuel cell, *International Journal of Hydrogen Energy*, 35 (2010) 13088-13095.

[23] Y.-H. Su, Y.-L. Liu, Y.-M. Sun, J.-Y. Lai, D.-M. Wang, Y. Gao, B. Liu, M.D. Guiver, Proton exchange membranes modified with sulfonated silica nanoparticles for direct methanol fuel cells, *Journal of Membrane Science*, 296 (2007) 21-28.

[24] H. Zhang, X. Li, C. Zhao, T. Fu, Y. Shi, H. Na, Composite membranes based on highly sulfonated PEEK and PBI: Morphology characteristics and performance, *Journal of Membrane Science*, 308 (2008) 66-74.

- [25] J.G. Hong, Y. Chen, Nanocomposite reverse electrodialysis (RED) ion-exchange membranes for salinity gradient power generation, *Journal of Membrane Science*, 460 (2014) 139-147.
- [26] M. Arsalan, M.M.A. Khan, Rafiuddin, A comparative study of theoretical, electrochemical and ionic transport through PVC based $\text{Cu}_3(\text{PO}_4)_2$ and polystyrene supported $\text{Ni}_3(\text{PO}_4)_2$ composite ion exchange porous membranes, *Desalination*, 318 (2013) 97-106.
- [27] X. Zuo, S. Yu, X. Xu, R. Bao, J. Xu, W. Qu, Preparation of organic–inorganic hybrid cation-exchange membranes via blending method and their electrochemical characterization, *Journal of Membrane Science*, 328 (2009) 23-30.
- [28] K. Hu, T. Xu, W. Yang, Y. Fu, Preparation of novel heterogeneous cation-permeable membranes from blends of sulfonated poly(phenylene sulfide) and poly(ether sulfone), *Journal of Applied Polymer Science*, 91 (2004) 167-174.
- [29] K. Hu, T. Xu, Y. Fu, W. Yang, Preparation of novel semihomogeneous cation-permeable membranes from blends of sulfonated poly(phenylene sulfide) and sulfonated phenolphthalein poly(ether ether ketone), *Journal of Applied Polymer Science*, 92 (2004) 1478-1485.
- [30] J. Rozière, D.J. Jones, NON-FLUORINATED POLYMER MATERIALS FOR PROTON EXCHANGE MEMBRANE FUEL CELLS, *Annual Review of Materials Research*, 33 (2003) 503-555.
- [31] K.A. Mauritz, Organic-inorganic hybrid materials: perfluorinated ionomers as sol-gel polymerization templates for inorganic alkoxides, *Materials Science and Engineering: C*, 6 (1998) 121-133.
- [32] M.M.A. Khan, Rafiuddin, Preparation and study of the electrochemical properties of magnesium phosphate membranes, *Journal of Applied Polymer Science*, 124 (2012) E338-E346.
- [33] P. Długołęcki, K. Nymeijer, S. Metz, M. Wessling, Current status of ion exchange membranes for power generation from salinity gradients, *Journal of Membrane Science*, 319 (2008) 214-222.
- [34] J. Veerman, R. De Jong, M. Saakes, S. Metz, G. Harmsen, Reverse electrodialysis: Comparison of six commercial membrane pairs on the thermodynamic efficiency and power density, *Journal of Membrane Science*, 343 (2009) 7-15.
- [35] R. Audinos, Electrodialyse inverse. Etude de l'energie electrique obtenue a partir de deux solutions de salinites differentes, *Journal of Power Sources*, 10 (1983) 203-217.

- [36] R. Audinos, Ion-Exchange membrane processes for clean industrial chemistry, *Chemical Engineering & Technology*, 20 (1997) 247-258.
- [37] M. Turek, B. Bandura, Renewable energy by reverse electrodialysis, *Desalination*, 205 (2007) 67-74.
- [38] P. Długołęcki, P. Ogonowski, S.J. Metz, M. Saakes, K. Nijmeijer, M. Wessling, On the resistances of membrane, diffusion boundary layer and double layer in ion exchange membrane transport, *Journal of Membrane Science*, 349 (2010) 369-379.
- [39] A. Daniilidis, R. Herber, D.A. Vermaas, Upscale potential and financial feasibility of a reverse electrodialysis power plant, *Applied Energy*, 119 (2014) 257-265.
- [40] W. Li, W.B. Krantz, E.R. Cornelissen, J.W. Post, A.R.D. Verliefde, C.Y. Tang, A novel hybrid process of reverse electrodialysis and reverse osmosis for low energy seawater desalination and brine management, *Applied Energy*, 104 (2013) 592-602.
- [41] R. Pattle, Production of electric power by mixing fresh and salt water in the hydroelectric pile, (1954).
- [42] F. Helfer, C. Lemckert, Y.G. Anissimov, Osmotic power with Pressure Retarded Osmosis: Theory, performance and trends—A review, *Journal of Membrane Science*, 453 (2014) 337-358.
- [43] S. Koter, P. Piotrowski, J. Kerres, Comparative investigations of ion-exchange membranes, *J Membrane Sci*, 153 (1999) 83-90.
- [44] J. Post, C. Goeting, J. Valk, S. Goinga, J. Veerman, H. Hamelers, P. Hack, Towards implementation of reverse electrodialysis for power generation from salinity gradients, *Desalination and water treatment*, 16 (2010) 182-193.
- [45] F. Wilhelm, N. Van der Vegt, H. Strathmann, M. Wessling, Comparison of bipolar membranes by means of chronopotentiometry, *Journal of membrane science*, 199 (2002) 177-190.
- [46] B. Kosmala, J. Schauer, Ion - exchange membranes prepared by blending sulfonated poly (2, 6 - dimethyl - 1, 4 - phenylene oxide) with polybenzimidazole, *Journal of applied polymer science*, 85 (2002) 1118-1127.
- [47] T. Xu, D. Wu, L. Wu, Poly (2, 6-dimethyl-1, 4-phenylene oxide)(PPO)—a versatile starting polymer for proton conductive membranes (PCMs), *Progress in Polymer Science*, 33 (2008) 894-915.

- [48] S. Zhang, T. Xu, C. Wu, Synthesis and characterizations of novel, positively charged hybrid membranes from poly (2, 6-dimethyl-1, 4-phenylene oxide), *Journal of membrane science*, 269 (2006) 142-151.
- [49] G.M. Geise, M.A. Hickner, B.E. Logan, Ionic Resistance and Permselectivity Tradeoffs in Anion Exchange Membranes, *ACS Applied Materials & Interfaces*, 5 (2013) 10294-10301.
- [50] P. Zschocke, D. Quellmalz, Novel ion exchange membranes based on an aromatic polyethersulfone, *Journal of Membrane Science*, 22 (1985) 325-332.
- [51] S. Yang, C. Gong, R. Guan, H. Zou, H. Dai, Sulfonated poly(phenylene oxide) membranes as promising materials for new proton exchange membranes, *Polymers for Advanced Technologies*, 17 (2006) 360-365.
- [52] H. Fu, L. Jia, J. Xu, Studies on the sulfonation of poly(phenylene oxide) (PPO) and permeation behavior of gases and water vapor through sulfonated PPO membranes. I. Sulfonation of PPO and characterization of the products, *Journal of Applied Polymer Science*, 51 (1994) 1399-1404.
- [53] K. Saito, K. Saito, K. Sugita, M. Tamada, T. Sugo, Convection-aided collection of metal ions using chelating porous flat-sheet membranes, *Journal of Chromatography A*, 954 (2002) 277-283.
- [54] Y. Wu, C. Wu, T. Xu, X. Lin, Y. Fu, Novel silica/poly (2, 6-dimethyl-1, 4-phenylene oxide) hybrid anion-exchange membranes for alkaline fuel cells: effect of heat treatment, *Journal of Membrane Science*, 338 (2009) 51-60.
- [55] C. DeMerlis, D. Schoneker, Review of the oral toxicity of polyvinyl alcohol (PVA), *Food and Chemical Toxicology*, 41 (2003) 319-326.
- [56] Z. Pan, C. Wu, J. Liu, W. Wang, J. Liu, Study on mechanical properties of cost-effective polyvinyl alcohol engineered cementitious composites (PVA-ECC), *Construction and Building Materials*, 78 (2015) 397-404.
- [57] J.S. Park, J.W. Park, E. Ruckenstein, A dynamic mechanical and thermal analysis of unplasticized and plasticized poly (vinyl alcohol)/methylcellulose blends, *Journal of applied polymer science*, 80 (2001) 1825-1834.
- [58] J. Zhang, J. Qiao, G. Jiang, L. Liu, Y. Liu, Cross-linked poly(vinyl alcohol)/poly (diallyldimethylammonium chloride) as anion-exchange membrane for fuel cell applications, *Journal of Power Sources*, 240 (2013) 359-367.
- [59] Y. Xiong, Q.L. Liu, Q.G. Zhang, A.M. Zhu, Synthesis and characterization of cross-

linked quaternized poly(vinyl alcohol)/chitosan composite anion exchange membranes for fuel cells, *Journal of Power Sources*, 183 (2008) 447-453.

[60] M.I. Baker, S.P. Walsh, Z. Schwartz, B.D. Boyan, A review of polyvinyl alcohol and its uses in cartilage and orthopedic applications, *Journal of Biomedical Materials Research Part B: Applied Biomaterials*, 100 (2012) 1451-1457.

[61] D.L. Feldheim, D.R. Lawson, C.R. Martin, Influence of the sulfonate counteraction on the thermal stability of nafion perfluorosulfonate membranes, *Journal of Polymer Science Part B: Polymer Physics*, 31 (1993) 953-957.

[62] Y.-W. Chang, E. Wang, G. Shin, J.-E. Han, P.T. Mather, Poly(vinyl alcohol) (PVA)/sulfonated polyhedral oligosilsesquioxane (sPOSS) hybrid membranes for direct methanol fuel cell applications, *Polymers for Advanced Technologies*, 18 (2007) 535-543.

[63] Y. Wu, J. Hao, C. Wu, F. Mao, T. Xu, Cation exchange PVA/SPPO/SiO₂ membranes with double organic phases for alkali recovery, *Journal of Membrane Science*, 423 (2012) 383-391.

[64] J. Qiao, J. Fu, L. Liu, Y. Liu, J. Sheng, Highly stable hydroxyl anion conducting membranes poly (vinyl alcohol)/poly (acrylamide-co-diallyldimethylammonium chloride)(PVA/PAADDA) for alkaline fuel cells: Effect of cross-linking, *international journal of hydrogen energy*, 37 (2012) 4580-4589.

[65] J. Zhang, J. Qiao, G. Jiang, L. Liu, Y. Liu, Cross-linked poly (vinyl alcohol)/poly (diallyldimethylammonium chloride) as anion-exchange membrane for fuel cell applications, *Journal of Power Sources*, 240 (2013) 359-367.

[66] J.-W. Rhim, H.B. Park, C.-S. Lee, J.-H. Jun, D.S. Kim, Y.M. Lee, Crosslinked poly (vinyl alcohol) membranes containing sulfonic acid group: proton and methanol transport through membranes, *Journal of Membrane Science*, 238 (2004) 143-151.

[67] N. Seeponkai, J. Wootthikanokkhan, Proton conductivity and methanol permeability of sulfonated poly(vinyl alcohol) membranes modified by using sulfoacetic acid and poly(acrylic acid), *Journal of Applied Polymer Science*, 105 (2007) 838-845.

[68] R.K. Nagarale, G.S. Gohil, V.K. Shahi, Recent developments on ion-exchange membranes and electro-membrane processes, *Adv Colloid Interfac*, 119 (2006) 97-130.

[69] H. Strathmann, Ion-exchange membrane separation processes, Elsevier, Amsterdam, Boston, 2004.

[70] <Cation permeable membranes from blends of sulfonated poly(ether ether ketone) and poly(ether sulfone).pdf>.

- [71] H. Strathmann, A. Grabowski, G. Eigenberger, Ion-Exchange Membranes in the Chemical Process Industry, *Industrial & Engineering Chemistry Research*, 52 (2013) 10364-10379.
- [72] P. Dlugolecki, K. Nymeijer, S. Metz, M. Wessling, Current status of ion exchange membranes for power generation from salinity gradients, *Journal of Membrane Science*, 319 (2008) 214-222.
- [73] R.K. Nagarale, G.S. Gohil, V.K. Shahi, Recent developments on ion-exchange membranes and electro-membrane processes, *Advances in colloid and interface science*, 119 (2006) 97-130.
- [74] A.H. Galama, J.W. Post, M.A. Cohen Stuart, P.M. Biesheuvel, Validity of the Boltzmann equation to describe Donnan equilibrium at the membrane–solution interface, *Journal of Membrane Science*, 442 (2013) 131-139.
- [75] C. Klaysom, S.H. Moon, B.P. Ladewig, G.Q.M. Lu, L.Z. Wang, Preparation of porous ion-exchange membranes (IEMs) and their characterizations, *J Membrane Sci*, 371 (2011) 37-44.
- [76] S. Koter, Influence of the layer fixed charge distribution on the performance of an ion-exchange membrane, *Journal of Membrane Science*, 108 (1995) 177-183.
- [77] T.-J. Chou, A. Tanioka, Ionic behavior across charged membranes in methanol–water solutions. I: Membrane potential, *Journal of Membrane Science*, 144 (1998) 275-284.
- [78] S. Gu, R. Cai, T. Luo, Z. Chen, M. Sun, Y. Liu, G. He, Y. Yan, A Soluble and Highly Conductive Ionomer for High - Performance Hydroxide Exchange Membrane Fuel Cells, *Angewandte Chemie International Edition*, 48 (2009) 6499-6502.
- [79] R.E. Lacey, Energy by reverse electrodialysis, *Ocean Engineering*, 7 (1980) 1-47.